

Fig. 1 A comparison of model magnetic field profiles with that observed by the Giotto magnetometer during the outbound pass of comet Halley¹. The case of constant $n(r)$ (a, plain broken line) provides the better fit to the observed profile than when $n(r) \propto 1/r$ (b, dotted broken line), but this could be partly a consequence of the fact that the pass was transverse to rather than along the comet-Sun direction. To fit the location of the magnetic field cut-off ($r_0 \approx 3,800$ km) and the peak field value ($B_m \approx 65$ nT), it is required that $Q = 1.1 \times 10^{30}$ molecules s^{-1} in case (a) (photochemical equilibrium) and $n_i = 6,000$ cm^{-3} with the same value of Q in case (b). Note the S/C event time is in UT.

occur at a distance of about 2,000 km if $B_m = 90$ nT and at about 4,500 km if $B_m = 60$ nT.

The values of the various parameters we have used are not precise and any coincidence with the observed magnetic field configuration in the vicinity of the ionopause is to some extent accidental. However, it is possible to match the observations rather well, as Fig. 1 indicates, where the parameters have been adjusted so that the correct values of r_0 and B_m are achieved. The assumption that $n(r)$ is constant provides the better fit and is more consistent with the observed ion density distribution^{7,8}.

We have neglected the plasma pressure in the above, but this can be included provided that the temperature is known, or can be determined separately. Thus (1) should be modified to

$$j = en(R_e + R_i)W - (1/B) \partial P / \partial r \quad (7)$$

where $P = nk(T_i + T_e)$ is the pressure, k is Boltzmann's constant and T_i and T_e are the ion and electron temperatures, respectively. For a given $P = P(r)$, we can integrate (7) and obtain a modified form for the magnetic field. In particular, if $P(r) = P_1$ for $B = 0$ and $P(r) = P_2$ otherwise, with $P_1 > P_2$, then the solution proceeds as before but the ionopause occurs where $B^2/8\pi = P_1 - P_2$ as would be expected. In the limit, where the effects of friction are negligible, the solution is easily found to be $B = B_m(r_m/r)H(r - r_m)$, with $H(r)$ the step function and $B_m^2/8\pi = P_1 - P_2$. One can allow for more general forms for $P(r)$ but this is of little value unless an appropriate model is used, in particular for T_e ⁹.

We suggest that the ionopause observed surrounding the nucleus of comet Halley must have been principally the result of friction² rather than a difference in plasma pressure^{3,4}. This is supported by the good qualitative and even quantitative agreement outlined above and also the apparent macroscopic stability of the observed structure and the difficulty of accounting for the necessary pressure difference required otherwise. An ionopause determined by pressure balance alone is highly susceptible to Kelvin-Helmholtz and Rayleigh-Taylor instabilities, which should lead to an irregular and diffuse boundary with internal 'flux ropes' as seen at Venus, for example¹⁰. The stability analyses made so far do not allow for photochemical and compressibility effects, which could be of some significance, but

most importantly they do not allow for the effects of friction self-consistently in the configuration before it is disturbed^{11,12}. We have not yet succeeded in finding any instability of the configuration described by (4) or (6) and note that even on the microscopic level little is to be expected as the differences in the electron and ion drift motions contributing to j are comparable with the ion acoustic wave speed, for example, only in a region about 1 km thick where the field is weak and the current is a maximum.

To make a significant contribution to the overall stress balance the plasma pressure and especially the pressure differences must be of order $B_m^2/8\pi$. With $B_m \approx 60$ nT this implies that the product $n(T_e + T_i)$ must be $\sim 10^8$ K cm^{-3} . With the above values for the parameters involved, the assumption of photochemical equilibrium suggests that the plasma number density at the ionopause was about 3,000 cm^{-3} , requiring a rather high electron temperature of about 30,000 K, assuming that $T_i \approx 300$ K as expected and as indicated by the observations⁷. In fact there is no direct information about the value of nT_e but it is reasonable to assume that the electron temperature within the ionopause is less than that in the region surrounding it because the density of neutrals, which are the main cause of electron cooling, is greater. Because there is also little change in the plasma density across the boundary of the diamagnetic cavity^{7,8}, it is difficult to see how plasma pressure differences could provide the desired effect. Based on existing models⁹ we would in fact expect the plasma pressure to be an order of magnitude less than the observed $B_m^2/8\pi$.

Note added in proof: After submission of the original manuscript we learnt that T. E. Craven, in an independent work (*Adv. Space Res.*, in the press), had obtained a solution in part similar to the present model.

Received 30 June; accepted 4 November 1986.

1. Neubauer, F. M. *et al. Nature* **321**, 352-355 (1986).
2. Ip, W.-H. & Axford, W. I. in *Comets* (ed. Wilkening, L. L.) 588-634 (University of Arizona Press, Tucson, 1982).
3. Schmidt, H. U. & Wegman, R. in *Comets* (ed. Wilkening, L. L.) 538-560 (University of Arizona Press, Tucson, 1982).
4. Wallis, M. K. & Dryer, M. *Astrophys. J.* **205**, 895-899 (1976).
5. Axford, W. I., Cunnold, D. M. & Gleeson, L. J. *Planet. Space Sci.* **14**, 909-919 (1966).
6. Riedler, W., Schwingenschuh, K., Yeroshenko, Ye. G., Styashkin, V. A. & Russell, C. T. *Nature* **321**, 288-299 (1986).
7. Balsiger, H. *et al. Nature* **321**, 330-334 (1986).
8. Krankowsky, D. *et al. Nature* **321**, 326-329 (1986).
9. Mendis, D. A., Houppis, H. L. F. & Marconi, M. L. *Fundamentals cosm. Phys.* **10**, 1-380 (1985).
10. Elphic, R. C. *et al. J. geophys. Res.* **85**, 7679 (1980).
11. Galeev, A. A. & Lipatov, A. S. *Adv. Space Res.* **4**, 229-257 (1984).
12. Ershkovich, A. I. & Mendis, D. A. *Astrophys. J.* **302**, 849 (1986).

Atomic-scale surface modifications using a tunnelling microscope

R. S. Becker, J. A. Golovchenko & B. S. Swartzentruber

AT&T Bell Laboratories, Murray Hill, New Jersey 07974, USA

The desire to modify materials on the smallest possible scale is motivated by goals ranging from high-density information storage to the purposeful transformation of genetic material. Here we report an atomic-scale modification of the surface of a nearly perfect germanium crystal, effected by the tungsten tip of a tunnelling microscope. We believe this to be the smallest spatially controlled, purposeful transformation yet impressed on matter and we argue that the limit set by the discreteness of atomic structure has now essentially been reached.

Significant progress in the field of surface physics over the past 25 years has provided the tools (ultra-high-vacuum (UHV) environments, argon-ion sputtering, low-energy electron diffraction, Auger electron spectroscopy) to prepare crystal surfaces in a chemically pure and structurally homogeneous state. This homogeneity is manifest as a nearly perfect, periodic, two-

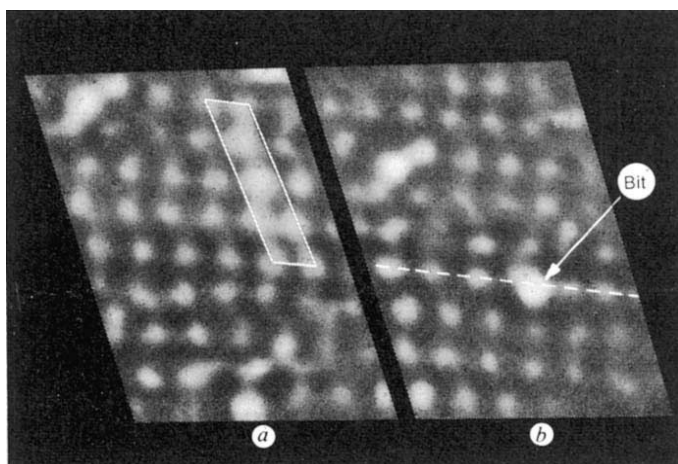


Fig. 1 Tunnelling images of a reconstructed (111) germanium surface covering a $50 \times 65 \text{ \AA}$ region. *a*, The surface before modification. A single unit cell of the $c\text{-}(2 \times 8)$ reconstruction is highlighted and a naturally occurring defect in the upper left hand corner serves as a registration mark. *b*, The same region after the surface modification. The displayed region is slightly translated due to thermal drift in the tunnelling microscope. The new bright spot near the centre of the picture is the impressed bit.

dimensional atomic array. The method of modifying the surface on an atomic scale is an extension of our recent studies of the electrical properties of semiconductor surfaces using a tunnelling microscope. A complete understanding of the procedures that have been effective requires further discussion of the instrument^{1,2}. The tunnelling microscope consists of a fine tungsten needle mounted on a set of piezoelectrically controlled manipulators. The ultimate resolution that may be obtained with the instrument (\sim several angstroms) indicates that the needle's tip is terminated by a few or perhaps even just a single atom. The manipulators are capable of moving the needle in all three dimensions continuously with fine control of 0.1 \AA .

The distance between the tip and a sample surface is maintained by one of these manipulators which is controlled by a feedback network. This feedback network senses the small tunnelling current induced to flow across the atomic-scale gap between tip and sample by a small bias voltage, compares that value with a desired reference and uses the time-integrated error signal to drive the piezo manipulator to adjust the gap so that the tunnel and reference current agree. Knowledge of the piezo manipulator calibration constant, in angstroms per volt, together with the closed-loop integrated error signal applied to it, determines the actual tip position in a direction normal to the surface. When desired, lateral motion of the tip across the surface is simply adjusted with two orthogonal non-servo controlled piezoelectric transducers. A tunnelling image of a surface is a

display of the feedback-controlled tip height as a function of its lateral position.

Detailed studies of the electrical properties of the tip-sample tunnel junction can be informative in attempts to interpret the tunnelling images obtained with the microscope³. While extending these studies to the case of the germanium surface we discovered that certain bias conditions resulted in a stable transformation in the atomic structure of the surface just below the tip. The transformation, controlled, localized and on an atomic scale, is the transformation we referred to above.

Figure 1*a* shows a tunnelling image of UHV-prepared Ge(111) surface before transformation. The tip was biased at -1.0 V relative to the sample and a tunnelling current of 20 pA was used. The data are displayed as a grey scale map where each lateral data point is represented by a corresponding pixel and the grey level of each pixel has been mapped from the recorded tip height. Light regions are higher (the tip had to withdraw to maintain 20 pA of tunnel current) than dark ones. Figure 1 corresponds to a region $50 \times 65 \text{ \AA}$ in lateral extent most of which is covered by the $c\text{-}(2 \times 8)$ reconstruction⁴. A unit cell is indicated in Fig. 1*a*. Also seen are naturally occurring isolated defects where the periodicity of the surface lattice is broken. The imperfection in the upper left-hand corner will serve as a reference or registration marker below.

The essentially perfect central region of the Fig. 1 was chosen as the place to write an atomic-scale 'bit'. This was accomplished by raising the tip to surface bias to -4.0 V at a quiescent tunnel current of 20 pA while the tip remained laterally stationary over the site chosen for modification. Successful modification of the surface is indicated electrically by a rapid withdrawal of the tip from the surface by $\sim 1 \text{ \AA}$. The bias was then reduced to the value used for taking tunnelling topographs ($\sim 1 \text{ V}$) and an image, shown in Fig. 1*b*, of the entire region surrounding the impressed bit was obtained by the same procedure used to obtain Fig. 1*a*. The same naturally occurring disruption of the lattice periodicity in Fig. 1*a* may be easily identified and used to register the two images relative to one another. The main feature of interest is the small isolated new protrusion in a previously pristine region of the surface. This transformation, indicated by the arrow in Fig. 1*b*, is the smallest spatial rearrangement of surface atoms we have observed to date.

The scale of the transformation can be appreciated in Fig. 2 which shows before and after plots of the surface height along the line shown in Fig. 1*b* which passes directly through the bit position. The small modulations characteristic of the undisturbed surface crystallinity in Fig. 2*a* are augmented by a 1-\AA high bump with a full width at half maximum of 8 \AA in Fig. 2*b*.

Figure 3 shows a plot of the typical electromechanical behaviour of the tip-sample tunnel junction with the feedback loop closed and a demanded tunnel current of 20 pA . The general character of the curves reflects the fact that, for increasing bias, the tip must be withdrawn to maintain constant tunnel current. Curve *ab* corresponds to a voltage scan where no transformation of the surface was induced. Curve *acde* shows

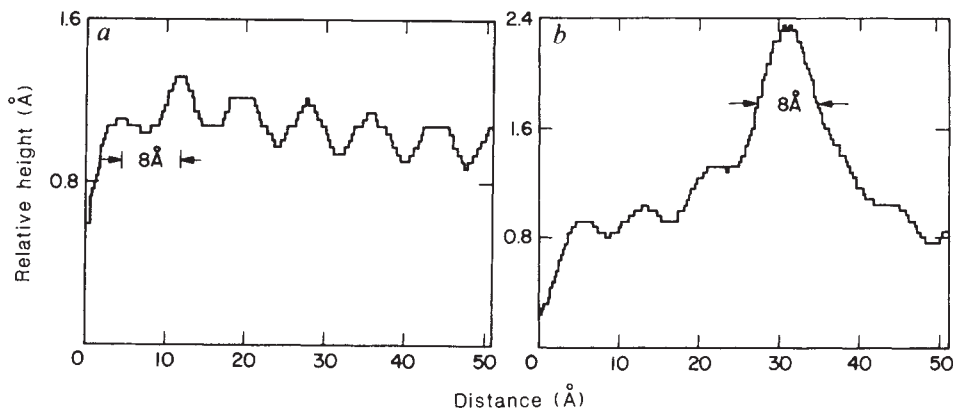


Fig. 2 Scan of the surface height: *a*, before; *b*, after impression of the bit. The scan is along the dotted line in Fig. 1*b* which passes through the bit position.

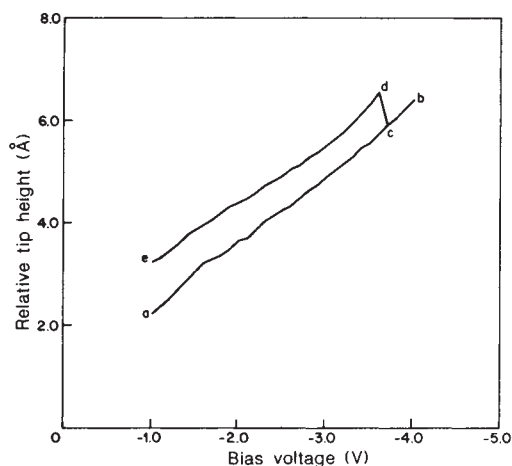


Fig. 3 Electromechanical junction response.

the situation under which an irreversible transformation was induced at *c* corresponding to a tip withdrawal of 1 Å *cd* which is maintained as the voltage is reduced *de*.

A few additional experimental observations are relevant to the discussion. First, we have never observed the transformation described above on silicon (111) surfaces even though tunnel currents were increased to several nanoamps and bias voltages as high as 20 V were used. Second, although this transformation could be repeated at different places on the surface not every attempt was successful. In some experiments, >90% of the attempts were successful and in others <10% were. The success rate improved when the tip was 'recharged' by taking it to a far-removed place on the surface and bringing it into contact with the surface.

Because the bit appears as added matter above the surface, one immediately questions its origin. One possibility is the tip itself. Germanium atoms previously transferred to the tungsten tip by contact with the sample may be redeposited under the electrical stimulation⁵ described above. Note that whereas stable silicides of tungsten exist, no germanium tungsten alloys are known. Germanium atoms may, therefore, be much less tightly bonded to the tungsten tip than silicon which would account for the success on germanium surfaces. It also seems reasonable to attribute the variability of results to variability in the state of the unobserved and poorly characterized tip rather than the uniform sample surface. The ability to recharge the tip also suggests it is the matter source. On the other hand, a reconfiguration of atoms of the equilibrium surface reconstruction may be stimulated by the high fields and current densities involved. We prefer the former explanation for the data and will discuss this in detail elsewhere. Nevertheless we believe the second mechanism may have an important role under appropriate circumstances.

We are uncertain about the actual atomic structure of the surface bit. In particular, the observed lateral dimension is certainly an upper limit to the actual size as the tunnelling images are a kind of convolution between the tip and surface geometry. To complicate matters the explanation for the unmodified $c-(2 \times 8)$ germanium surface is not completely understood so the details of the bit structure are difficult to anticipate. The understanding of nonequilibrium surface defect structures of the type we have induced represent a major new challenge to the materials and surface physics community.

We are convinced that a new rich field lies ahead in the study of atomic-sized structures on surfaces (see refs 6 and 7). The final rewards may be high-density memories, new devices whose electrical properties are dominated by quantum-size effects, or the modifications of a single self-replicating molecule on a surface. Such endeavours will require a much more elaborate understanding and control over materials and mechanisms than

we have demonstrated. Nevertheless, we hope to have shown that man can now manipulate a few chosen atoms for his own purposes.

Received 25 July; accepted 28 October 1986.

1. Binnig, G., Rohrer, H., Gerber, C. & Weibel, E. *Phys. Rev. Lett.* **50**, 120-123 (1983).
2. Golovchenko, J. A. *Science* **232**, 48-53 (1986).
3. Becker, R. S., Golovchenko, J. A., Hamann, D. R. & Swartzentruber, B. S. *Phys. Rev. Lett.* **55**, 2032-2034 (1985).
4. Becker, R. S., Golovchenko, J. A. & Swartzentruber, B. S. *Phys. Rev. Lett.* **55**, 2032-2034 (1985).
5. Hren, J. J. & Ranganathan, S. R. (eds) *Field Ion Microscopy* (Plenum, New York, 1968).
6. McCord, M. A. & Pease, R. F. W. *J. Vac. Sci. Technol.* **B4**, 86 (1986).
7. Ringger, M., Hidber, H. R., Schlögl, R., Oelhafen, P. & Guntherod, H.-J. *Appl. Phys. Lett.* **46**, 832 (1985).

Inertial waves identified in the Earth's fluid outer core

K. D. Aldridge & L. I. Lumb

Department of Earth and Atmospheric Science, York University, Toronto M3J 1P3, Canada

Several inertial waves have been identified in the long period gravimetric data of Melchior and Ducarme¹. These hydrodynamical waves which only exist because of the Earth's rotation, must be in the Earth's fluid outer core. Close proximity of the observed periods to those predicted for a homogeneous fluid suggests the waves should be labelled inertial because buoyancy and compressibility effects must be small or self-cancelling. Some of the identified waves have azimuthal wavenumber one, consistent with their occurrence after large, deep earthquakes which probably excite the waves through a small perturbation in the Earth's rotation. Other waves are axially symmetric, consistent with a small change in the magnitude of the fluid core's rotation rate. All the waves decay more rapidly than would be expected for Ekman dissipation which suggests an additional dynamical damping associated with mantle-inner core coupling. The inertial waves identified here will serve as a precise tool for subsequent evaluation of models for core dynamics and the geodynamo.

The region of the Earth between the depths of about 2,887 and 5,142 km defines the Earth's outer core, which has long been recognized to be a fluid. The oscillatory response of this slightly compressible, electrically conducting, nearly homogeneous, contained, rotating fluid to small, long period perturbations will be dominated by the Coriolis force. Such rotationally determined behaviour of a contained fluid produces what are known as inertial waves². Previous investigations of inertial waves have centred on meteorological and oceanographic applications, although they had been recognized much earlier³. Experimental investigations have been more recent with excitation and detection in cylindrical, spherical and conical cavities⁴⁻¹¹. Theoretical work on inertial waves has attracted attention partly because the ill-posed nature of the boundary value problem brings the existence of continuous solutions into question¹².

Recently geophysical interest has centred on the dynamics of a realistic fluid outer core taking into account compressibility, stratification and self-gravitation. Despite the mathematical complexity considerable progress has been made¹³⁻¹⁶. Since it is our expectation that the behaviour of the fluid core at the periods observed by Melchior and Ducarme will be dominated by rotation, we have chosen to model the core accordingly. Thus by introducing what might be called the Poincaré Earth model, we expect to find some small differences between our predicted eigenfrequencies and those already observed for the core. In future work these differences will be used to determine properties of the core.